2−5

HIGH ENTHALPY WORKSHOP PROBLEM II OREX

K. Murakami* and T. Fujiwara**
Nagoya University
Furou-cho Chikusa-ku Nagoya-shi 464-01, Japan
and
S. Nakano†
Hitachi Ltd.
3-1-1, Saiwai-cho, Hitachi-shi, Ibaraki-ken 317, Japan

Abstract

We have developed a CFD code to calculate a hypersonic flow around a reentry body including the base flow region. In order to inspect our CFD code we calculate Problem II OREX II-1, 2, 3 and 5 in this workshop. The problems II-1, 2 and 3 are laminar nonequilibrium gas flow. The result of Problem II-5 is used for the initial value of the reacting flow calculations of Problem II-2 and 3. For the thermally and chemically nonequilibrium flow calculations, 11-species air is considered, along with the Park's two-temperature model. For the calculation of flowfield, the governing equations are full Navier-Stokes ones and are solved using a non-MUSCL-type second-order explicit upwind-TVD scheme by Harten-Yee. For the problem II.1, 2 and 3, a semi-implicit method is applied to all species-mass-conservation-equations because of stiff source terms.

Introduction

Japanese first purely-national rocket, launched successfully 1994 February 4, carried an experimental reentry vehicle named OREX to orbit. The vehicle traveled at a hypersonic velocity in high altitudes where the air density is low. In this case, the flowfield behind the bow shock formed over the vehicle tends to be nonequilibrium chemically and thermally; the molecules N_2 and O_2 internally excite, dissociate and ionize in the shock layer and entailing downstream. Thus, we must consider internal excitation, dissociation and ionization. In other words, thermally- and chemically-nonequilibrium 11 species (O_2, N_2, O, N, NO, O_2^+, N_2^+, O^+, N^+, NO^+ and e^-) must generally be considered, using a model consisting of 17 chemical reactions and two temperatures, for example.

We have developed a CFD code to estimate the heat transfer on the surface of the reentry body like OREX because of its importance. In order to inspect our CFD code we participate High Enthalpy Flow Workshop and we calculate the Problem II OREX II-1, 2, 3 and 5. The flight conditions of OREX of these problems are shown in Table 1.

Mathematical Description of Hypersonic Flow

A system of governing equations that describe a three-dimensional, axisymmetric viscous flow of multi-component reacting air is given in terms of the cylindrical coordinate[1], after setting the angle of attack equal to zero; i.e. the equations are reduced to spacially two-dimensional system (r, z). We assume (a) the flow is in thermally non-equilibrium, (b) the radiation pressure and body forces are of negligible order, and (c) the molecular diffusion is binary only. These equations are then transformed into a general body-oriented curvilinear coordinate system (ξ, η), and then rearranged into a non-dimensional strong-conservation-form as follows:

$$\frac{\partial \hat{q}}{\partial \tau} + \frac{\partial \hat{E}}{\partial \xi} + \frac{\partial \hat{F}}{\partial \eta} = \frac{1}{Re}\left[\frac{\partial \hat{E}_v}{\partial \xi} + \frac{\partial \hat{F}_v}{\partial \eta}\right] + \hat{H} + \hat{H}_1, \quad (1)$$

where $\hat{H}$ and $\hat{H}_1$ are the mass production and cylindrical coordinate terms, respectively. When we are calculating 11-species flowfields using the Park 2-temperature model, we need one more equation, which is the vibrational energy conservation

$$\frac{\partial}{\partial t}(J^{-1}e_{ev}) + \frac{\partial}{\partial \xi}(J^{-1}e_{ev}U) + \frac{\partial}{\partial \eta}(J^{-1}e_{ev}V)$$

*Graduate Student, Department of Aerospace Engineering, Nagoya University.
**Professor, Department of Aerospace Engineering, Nagoya University.
†Researcher, 5th Department of Mechanical Engineering Research Laboratory, Hitachi Ltd.

$$= \frac{1}{Re}\left[\frac{\partial}{\partial\xi}J^{-1}\left(\xi_z Re\lambda\frac{\partial T_v}{\partial z}+\xi_r Re\lambda\frac{\partial T_v}{\partial r}\right)\right.$$
$$\left.+\frac{\partial}{\partial\eta}J^{-1}\left(\eta_z Re\lambda\frac{\partial T_v}{\partial z}+\eta_r Re\lambda\frac{\partial T_v}{\partial r}\right)\right]$$
$$-\frac{J^{-1}}{r}\left[(P_e+e_{ev})v-\lambda\frac{\partial T_v}{\partial r}\right]$$
$$+J^{-1}\left(3\gamma_e\sum_{i=1}^{6}\frac{m_e}{m_i}\theta_i+\frac{\gamma_m}{\tau}\right)\rho(T-T_v)$$
$$-P_e\left[\frac{\partial}{\partial\xi}\left(J^{-1}U\right)+\frac{\partial}{\partial\eta}\left(J^{-1}V\right)\right]. \qquad (2)$$

See the results of Park[2] for further information.

In order to consider a thermally- and chemically-nonequilibrium gas, a two-temperature model is used here: T indicates the translational and rotational temperature, while T_v the vibrational and electron temperature. When 11 chemical species (N_2, O_2, N, O, NO, N_2^+, O_2^+, N^+, O^+, NO^+ and e) are considered in the analysis, we utilize 17 chemical reactions shown in Table 2.

The forward k_f and backward k_b reaction rates of j-th reaction are given by the modified Arrhenius law as a function of T_a, which is defined in the two columns of Table 2:

$$k_f = CT_a{}^n exp(-E_1/kT_a), \quad k_b = k_f/K_c(T_a), \quad (3)$$

where the equilibrium constant Kc is given by the curve-fitting formula

$$K_c = exp(A_1 + A_2 \ln Z + A_3 Z + A_4 Z^2 + A_5 Z^3). \quad (4)$$

Here $Z = 10000/T_a$.

When the present two-temperature model is applied, the viscosity and thermal conductivity are calculated from the Yos formulation which is based on molecular collision cross section. Using the formulation, the following three thermal conductivities are introduced; (a) translational mode including the rotational energy, (b) vibrational mode, and (c) electron translational mode. The first is the function of the translational temperature T, while the others are of the vibrational temperature T_v. We can treat the thermal conduction of each mode separately. For more explanations, see Lee[3].

Calculation of Flowfield

For the calculation of flowfield, the governing equations (1) and (2) are solved using a non-MUSCL-type second-order explicit upwind-TVD scheme by Harten-Yee[4] and generalized Roe's average by Liu and Vinokur[5]. For the problem II.1, 2 and 3, a semi-implicit method is applied to all species-mass-conservation-equations because of stiff source terms.

Figure 1 is a typical example of body-oriented grid system. The grid system is generated by solving a hyperbolic equation. The minimum value of $\Delta\eta$ is 50 μm and the interval ratio between adjacent grids is limited below 1.04, therefore 150 points are needed for η direction. The innermost surface η=0 agrees with the body surface. The axis of symmetry is located in the center of two adjacent grid points. At the beginning of calculation the most outer boundary of calculation domain is set artificially. When the location of bow shock is almost fixed, the outer boundary and inner grid system are adjusted along the η direction. After that the flowfield calculation is continued. For each problem, this re-griding is done.

Results and Discussions

At first we calculate the perfect gas flow cases of Problem II-1 and 5 using the same CFD code for the perfect gas which is made up by ourselves. After we get converged solution of perfect gas, the nonequilibrium calculations are started from these solution as the initial inputs. The CFD code witch is used for the thermally and chemically nonequilibrium gas flow calculations is same for Problem II-1, 2 and 3 except for the initial input and free stream and wall conditions.

Figure 2 shows the dimensionless pressure contours. Since Problem II-1 is the low density and high speed case, the bow shock is spread in comparison with other cases. That effect of low density is seen from the dimensionless translational temperature contours Fig.3 and vibrational one Fig.4. We can see that in detail from Fig.7 which is the temperature distributions along the stagnation stream line.

The results of the heat transfer distributions along the body surface are shown in Fig.5. The wall heat transfers are calculated by following equation,

$$Q = -\left(\lambda\frac{\partial T}{\partial n}\right)_{wall} - \left(X_m\lambda_v\frac{\partial Tv}{\partial n}\right)_{wall}$$
$$-\left(X_e\lambda_e\frac{\partial Tv}{\partial n}\right)_{wall} - \sum_{i=1}^{Ns}\left(\rho_i h_i\frac{D_i}{Y_i}\frac{\partial Y_i}{\partial n}\right)_{wall} \quad (5)$$

The value of thermal conductivities of translational, vibrational and electronic excitation mode are listed in Table 3. Heat conduction by translational mode over body is calculated by Yos's formula and Wassilewas' formula for two-temperature model and non-reacting flow, respectively. In Eq.(??) n is normal vector to wall, then

$$\frac{\partial f}{\partial n} = \frac{(\eta_x\xi_x+\eta_y\xi_y)f_\xi+(\eta_x^2+\eta_y^2)f_\eta}{\sqrt{\eta_x^2+\eta_y^2}}. \quad (6)$$

where f is some physical value, f_ξ and f_η are calculated on wall by central-difference and foward-difference, respectively.

The maximum value of heat transfer along the body surface, however, becomes lower in all results of calculations. That lower estimate of heat transfer comes from the entropy fix of Harten-Yee type upwind-TVD scheme. The entropy fix is calculated by following equations.

$$\Psi(z) = \begin{cases} |z| & |z| \geq \delta \\ (z^2 + \delta^2)/2\delta & |z| < \delta \end{cases} \qquad (7)$$

$$\delta = \delta_1(|\xi_r u + \xi_z v| + a\sqrt{\xi_r^2 + \xi_z^2}) \qquad (8)$$

At the start point of calculation we set δ_1 equal to 1.0, and decrease to 0.1 finally. The constant δ_1 is used to all of the calculation domain. According to Eq.(8) the narrow the grid interval is, the smaller δ namely numerical viscosity becomes. Because of the sufficient numerical viscosity the temperature gradient near the body is made smaller. The effect of the numerical viscosity will be appeared in the distributions of mass fractions (Fig.6) near the surface. In order to estimate the heat transfer on the reentry body surface correctly we have to introduce some high-resolution method for boundary layer to our CFD code.

The vibrational temperature distributions along the stagnation stream line are shown in Fig.7. As seen from Fig.7 II-2, the vibrational temperature distribution has a sharp peak behind the shock front similar to translational one. It will come from that the electron pressure is ignored for simplicity when TVD scheme is applied to the system of governing equations which include the vibrational energy conservation. Therefore, we must re-examin the method for solving the vibrational energy conservation equation.

In the pressure and temperature contour Fig.2 and 3, there is something the matter with contour line around the axisymmetric line. According to our recent study, however, that is reduced by using the fractional step method for the calculations of two dimensional flow.

Conclusions

In this workshop, we can find several points that we must improve our CFD code to simulate a hypersonic thermally and chemically nonequilibrium gas flow around a reentry body like OREX. First, more higher resolution of boundary layer witch effect on the heat transfer along the body surface is need to estimate the heat transfer correctly. Second, when we consider the ionization and two temperature model we must re-examin the method for solving the vibrational energy conservation equation.

Further comparison between the results of numerical calculation and the experimental data is desirable after improvement of our CFD code in order to inspect its validity.

References

1) Kuo K.K. 1986, Principles of Combustion, John Wiley & Sons, pp.161-227.

2) Park C. 1985, Problems of rate chemistry in the flight regimes of aeroassisted orbital transfer vehicles, thermal design of aeroassisted orbital transfer vehicles, ed. H.F. Nelson, Progr. Astronaut. Aeronaut. 96, pp.511-537.

3) Lee J.H. 1985, Governing equations for the flight regimes of aeroassisted orbital transfer vehicles, thermal design of aeroassisted orbital transfer vehicles, ed. H.F. Nelson, Progr. Astronaut. Aeronaut. 96, pp.5-53.

4) Yee H.C. 1989, A class of high resolution explicit and implicit shock capturing methods, NASA TM 101088.

5) Liu Y. and Vinokur M. 1989, Upwind Algorithms for General Thermo-Chemical Nonequilibrium Flows, AIAA-89-0201.

Table 1: Flight conditions of OREX

	U_∞ [m/s]	T_∞ [K]	P_∞ [N/m^2]	T_{wall} [K]
II-1	7450	186.9	0.1629	540
II-2				
II-3	5562	248.1	23.60	1519
II-5				

Table 2: Elementary chemical reactions and temperature Ta contributing to each reaction rate

	k_f Ta	k_b Ta
$O_2 + M \rightleftarrows O + O + M$	$T^{1/2}T_v^{1/2}$	$T^{1/2}T_v^{1/2}$
$N_2 + M \rightleftarrows N + N + M$		
$NO + M \rightleftarrows N + O + M$		
$N_2 + O \rightleftarrows NO + N$	$T^{1/2}T_v^{1/2}$	$T^{1/2}T_v^{1/2}$
$NO + O \rightleftarrows N + O_2$		
$O + O_2^+ \rightleftarrows O_2 + O^+$	$T^{1/3}T_v{}^{2/3}$	$T^{1/3}T_v{}^{2/3}$
$N^+ + N_2 \rightleftarrows N_2^+ + N$		
$O + NO^+ \rightleftarrows NO + O^+$		
$N_2 + O^+ \rightleftarrows O + N_2^+$		
$N + NO^+ \rightleftarrows NO + N^+$		
$O_2 + NO^+ \rightleftarrows NO + O_2^+$		
$NO^+ + N \rightleftarrows N_2^+ + O$		
$O + N \rightleftarrows NO^+ + e^-$	$T^{1/2}T_v{}^{1/2}$	T_v
$O + O \rightleftarrows O_2^+ + e^-$		
$N + N \rightleftarrows N_2^+ + e^-$		
$O + e^- \rightleftarrows O^+ + e^- + e^-$	T_v	T_v
$N + e^- \rightleftarrows N^+ + e^- + e^-$		

Table 3: Value of thermal conductivities of translational, vibrational and electronic excitation mode

Problem	II-1	II-2
T_{wall} [K]	540	1519
λ [W/m/K]	3.942×10^{-2}	7.652×10^{-2}
$X_m\lambda_m$ [W/m/K]	2.537×10^{-3}	7.554×10^{-3}
$X_e\lambda_e$ [W/m/K]	7.650×10^{-7}	1.565×10^{-11}
Problem	**II-3**	**II-5**
T_{wall} [K]	1519	1519
λ [W/m/K]	7.663×10^{-2}	8.042×10^{-2}
$X_m\lambda_m$ [W/m/K]	1.860×10^{-2}	-
$X_e\lambda_e$ [W/m/K]	0.0	-

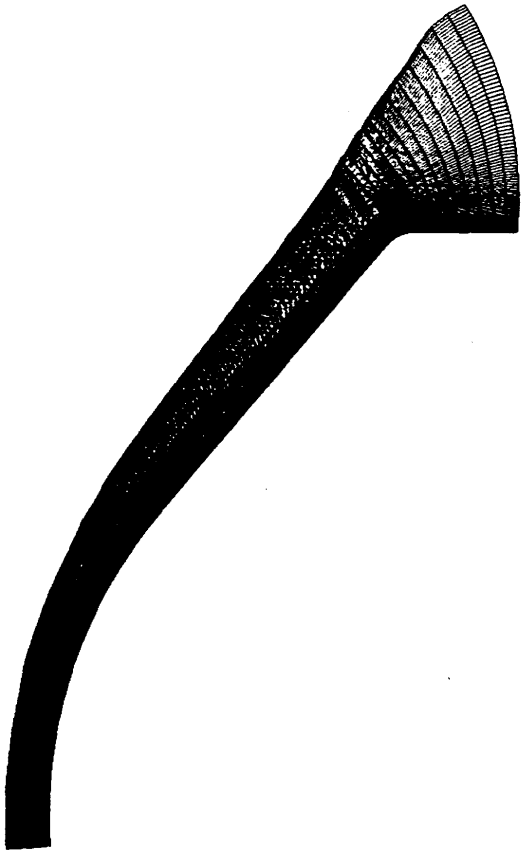

Figure 1: An example of body-oriented grid system. $\xi \times \eta = 51 \times 150$

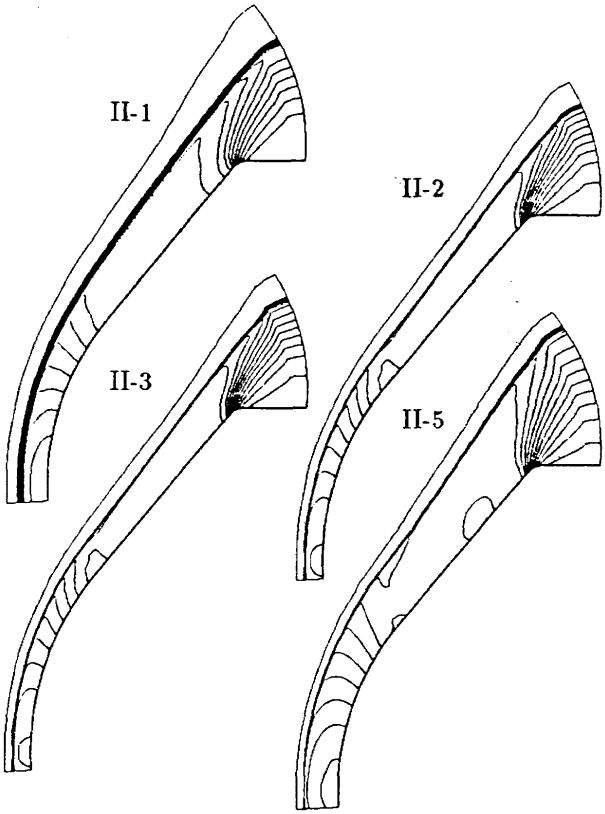

Figure 2: Dimensionless Pressure Contours

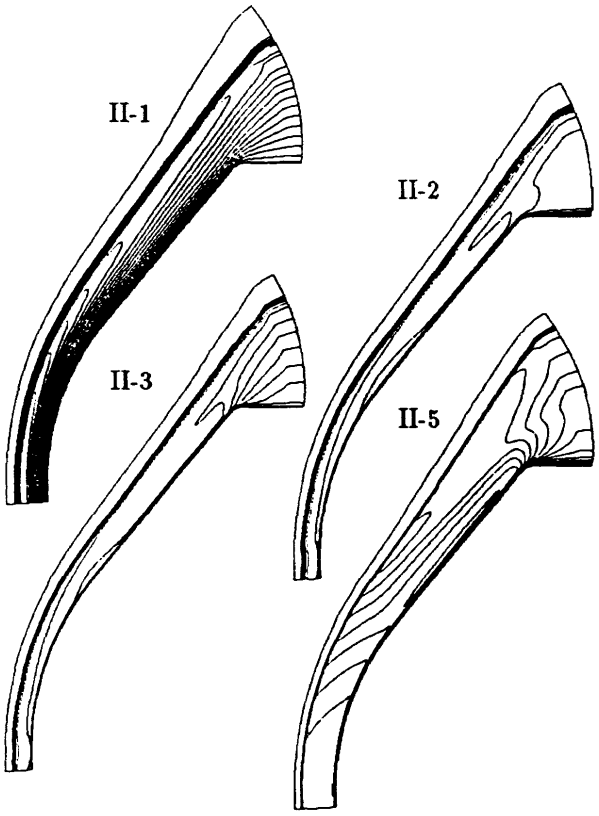

Figure 3: Dimensionless Translational Temperature Contours

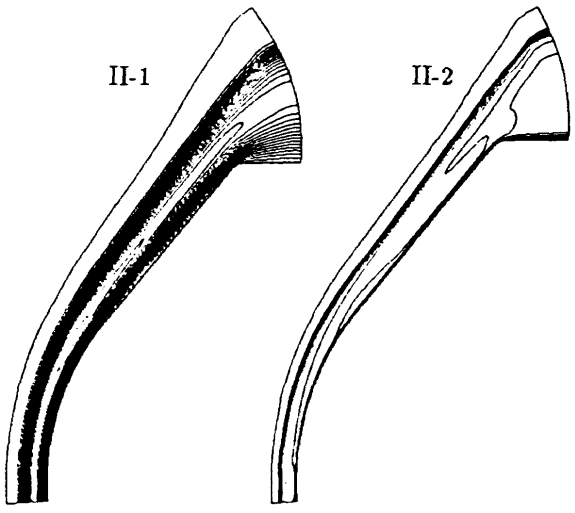

Figure 4: Dimensionless Vibrational Temperature Contours

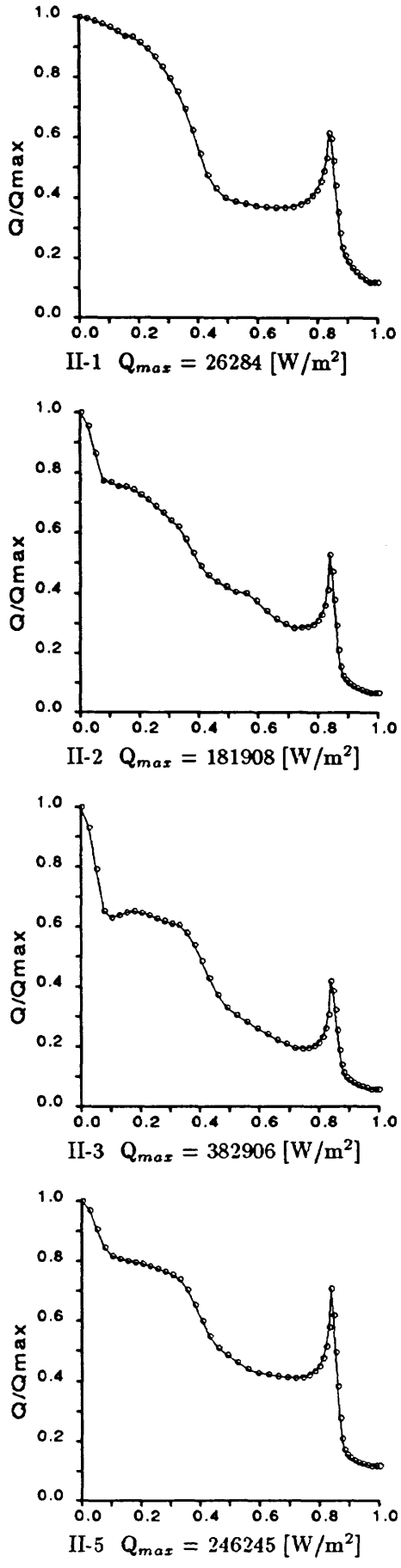

Figure 5: Heat Transfer Distribution along Body Surface

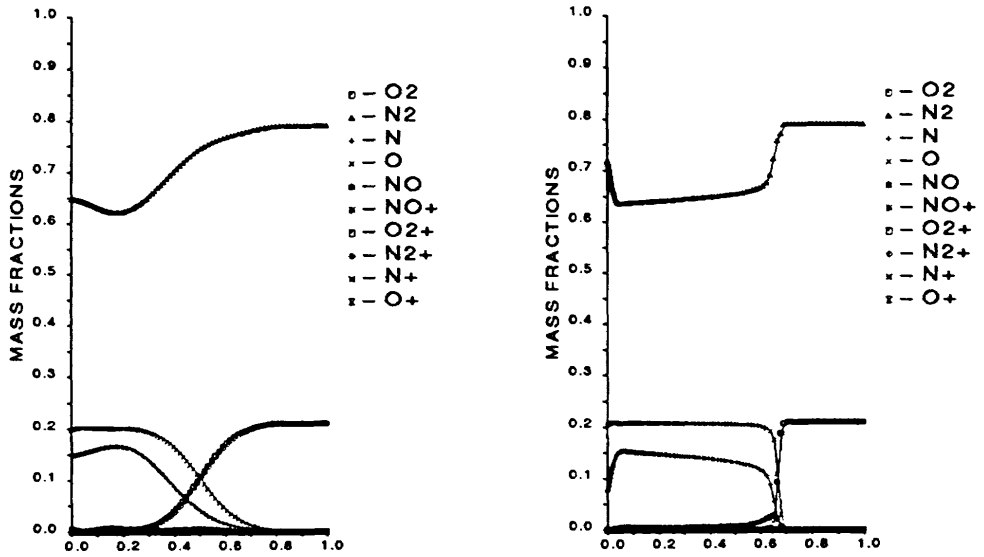

II-1 II-2

Figure 6: Mass Fraction Distribution along Stagnation Stream Line

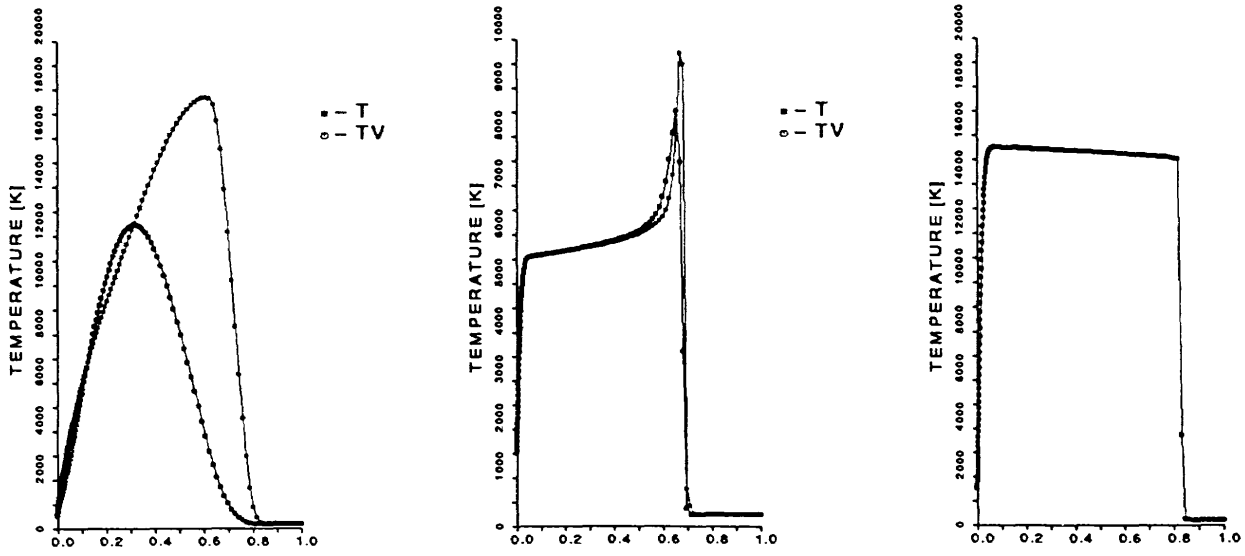

II-1 T_{max} = 17713 [K] TV_{max} = 12488 [K]

II-2 T_{max} = 9719 [K] TV_{max} = 8529 [K]

II-5 T_{max} = 15541 [K]

Figure 7: Temperature Distribution along Stagnation Stream Line